ARTICLES

Photodissociation Dynamics of *n*-Butylbenzene Molecular Ion

Seong Tae Oh, Joong Chul Choe,*,† and Myung Soo Kim*

Department of Chemistry and Center for Molecular Catalysis, Seoul National University, Seoul 151-742, Korea, and Department of Chemistry, University of Suwon, Kyunggi 445-743, Korea

Received: February 27, 1996[⊗]

Photodissociation dynamics of *n*-butylbenzene molecular ion has been investigated on a nanosecond time scale. The rate constants for production of $C_7H_8^{\bullet+}$ and $C_7H_7^+$, their branching ratios, and the kinetic energy release distributions have been determined by the photodissociation method using mass-analyzed ion kinetic energy spectrometry. The branching ratios have been found to be in excellent agreement with the previously established results. All the experimental data could be explained with statistical theories such as Rice−Ramsperger−Kassel−Marcus (RRKM) and phase space theories. RRKM fittings for these reactions have been improved. The present result supports the previous suggestion that the dissociation to $C_7H_8^{\bullet+}$ occurs via a stepwise McLafferty rearrangement.

1. Introduction

The kinetics of unimolecular ion dissociation has been a subject of general interest in chemistry and related fields. In particular, the successful interpretation of breakdown patterns in the mass spectra of polyatomic molecules with the quasi-equilibrium theory (QET) led to the establishment of mass spectrometry as a useful analytical technique.[1] The quasi-equilibrium theory, which is mathematically equivalent to the microcanonical Rice−Ramsperger−Kassel−Marcus (RRKM) theory for unimolecular dissociation, is usually referred to as RRKM-QET.[2,3] Breakdown patterns utilized to test RRKM-QET in the early days were basically determined by the relative magnitudes of rate constants of various reaction channels. Instead of these, measurement of the rate constant for the dissociation of energy-selected polyatomic ions would be more useful for the test of RRKM-QET and its application to the study of reaction mechanism. Some experimental techniques such as photoelectron−photoion coincidence (PEPICO) spectrometry[4] and photodissociation in ion cyclotron resonance (PD-ICR) spectrometer[5] have been developed for the above purpose. However, these techniques which have made tremendous contribution to the study of the kinetics and dynamics of unimolecular ion dissociation over the years allow rate constant measurement on milli- to microsecond time scale only. Recently, we have developed a technique[6] based on the mass-analyzed ion kinetic energy spectrometry (MIKES) of photodissociation products in a double-focusing mass spectrometer, namely PD-MIKES, which allows rate constant measurement on a nanosecond time scale. Hence, combining the rate−energy data available from the above techniques, it is now possible to investigate a unimolecular ion dissociation over 6 orders of magnitude in time scale. In addition to the rate constant, the kinetic energy release distribution (KERD) can be measured also with PEPICO and PD-MIKES, which provides useful information on the exit channel dynamics. This advantage has been utilized for the studies of dissociation of various molecular ions.[7−14] For example, non-RRKM nature in the dissociation of photoexcited *tert*-butylbenzene ion has been observed through PD-MIKES investigation.[12]

Dissociation of *n*-butylbenzene ion has been the focus of intensive research effort[15−28] ever since the pioneering ion-beam photodissociation experiments by Beynon and co-workers.[15−17] In particular, the branching ratio for the production of *m/z* 91 and 92 was found to depend sensitively on the photon energy, suggesting its use as a thermometer for determining the internal energy.

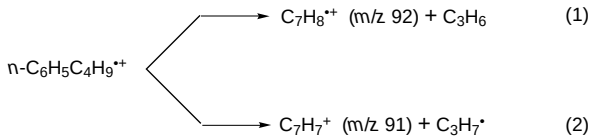

In fact, such a sensitive dependence is expected because the rate−energy dependences for the two reactions, reaction 1 occurring via a rearrangement (McLafferty) and reaction 2 occurring via a simple bond cleavage (α), are widely different. However, the above ion-beam results were found to be inconsistent with later investigations with charge exchange ionization by Harrison and Lin[19] and with PD-ICR by Dunbar and co-workers.[21] The latter investigators attempted an RRKM-QET fit to explain their 91/92 ratios and suggested that shifting the energy scale of the ion-beam results to higher energy by 1.5−2 eV would bring them into reasonable accord with other results. That is, this amount of energy would correspond to the internal energy of the parent ions being photoexcited.

The most detailed investigation so far on the kinetics and dynamics of *n*-butylbenzene ion dissociation has been carried out by Baer et al. using PEPICO.[27] The 91/92 branching ratio was measured over an internal energy range 2−6.5 eV, and the rate constant for the production of *m/z* 92 fragment ion was determined over a narrow internal energy range corresponding to rate constant of 10^5-10^6 s^{-1}. Even though the measured 91/92 ratios were in reasonable agreement with the charge exchange ionization[19,20] and PD-ICR[21] results, the rate constants were found to be larger by 2 orders of magnitude than predicted

* Authors to whom correspondence should be addressed.
† University of Suwon.
⊗ Abstract published in *Advance ACS Abstracts,* July 1, 1996.

S0022-3654(96)00581-3 CCC: $12.00

by Dunbar and co-workers.[21] An RRKM-QET fit of the above data was utilized to investigate the reactions. In particular, the stepwise occurrence of the McLafferty rearrangement leading to $92^{\bullet+}$ was inferred from the rate result together with the kinetic energy release data reported by Holmes and Osborne.[28]

Our instrumentation for PD-MIKES bears some resemblance to Beynon's,[15] even though details of the technique are quite different. Hence, we have felt it necessary to investigate the 91/92 ratio problem to see if the results are in accord with the results from well-established methods such as PEPICO. Also, nanosecond rate−energy data and KERD available from the present investigation have been utilized here to deepen our understanding of the kinetics and dynamics of reactions 1 and 2.

2. Experimental Section

The experimental setup has been described in detail elsewhere[6] and will be reviewed only briefly here. A double focusing mass spectrometer with reversed geometry (VG Analytical Model ZAB-E) modified for photodissociation study was used. *n*-Butylbenzene ions generated by charge exchange in the ion source and accelerated to 8 keV were mass-analyzed by the magnetic sector. Then, the ion beam was crossed with the laser beam in the field region of an electrode assembly located near the intermediate focal point of the instrument. The 607.5 nm output of a dye laser (Spectra Physics Model 375B) and the 514.5 and 488.0 nm lines of an argon ion laser (Spectra Physics Model 164-09) were used. The translational kinetic energy of the fragment ions was analyzed by the electric sector. This is called the mass-analyzed ion kinetic energy spectrometry. Since a MIKE spectrum contains contributions from metastable ion decomposition (MID) and collision-induced dissociation by residual gas, phase-sensitive detection was adopted to record a MIKE spectrum originating from photodissociation, namely, a PD-MIKE spectrum. To improve the quality of a MIKE spectrum, signal averaging was carried out for repetitive scans. Errors quoted in this work were estimated from several duplicate experiments at 95% confidence limits. For the photodissociation experiment, CS_2 was used as the reagent gas for charge exchange ionization. The ion source chamber was maintained at 140 °C. For the MID experiment, 70 eV electron ionization was used at an ion source temperature of 200 °C.

3. Results

It is well-known that the production of the *m/z* 92 ion dominates the dissociation of *n*-butylbenzene ion on a microsecond time scale.[27] In the MID-MIKE spectrum of *n*-butylbenzene ion recorded in this work, the *m/z* 92 peak has been found to constitute more than 97% of the total daughter ion. The *m/z* 91 ion was hardly observable as shown in Figure 1a. On the other hand, both the peaks at *m/z* 91 and 92 appear prominently in PD-MIKE spectra as shown in Figure 1b. The spectrum in the figure was recorded without the applied voltage on the electrode and is called a field-off PD-MIKE spectrum. Substantial noise appears at the *m/z* 92 position in this spectrum due to the presence of a strong metastable background, prohibiting a reliable determination of the branching ratio. This difficulty can be overcome by recording a field-on PD-MIKE spectrum, namely a spectrum obtained with a high voltage applied at the electrode assembly. Field-on PD-MIKE spectra with 1.5 kV applied voltage are shown in Figure 2. With the applied voltage, the PD-MIKE spectra tail toward lower translational energy, which is due to a distribution of time delay between photoexcitation and dissociation. The tailing is more severe with 607.5 nm excitation than with 488.0 nm because

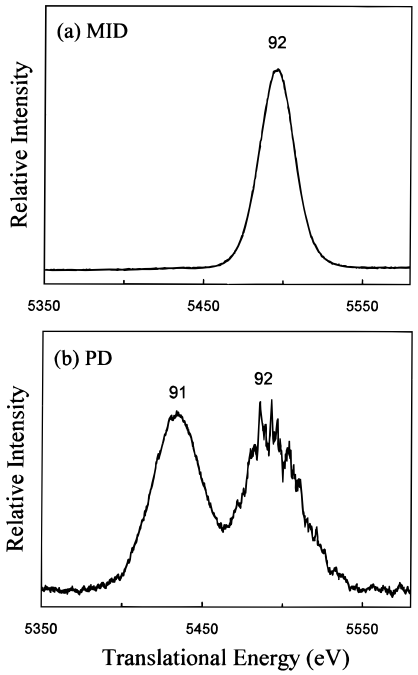

Figure 1. MIKE spectra for dissociation of *n*-butylbenzene ion: (a) metastable ion decomposition; (b) field-off photodissociation at 488.0 nm. *m/z* of the fragment ion corresponding to each peak is indicated.

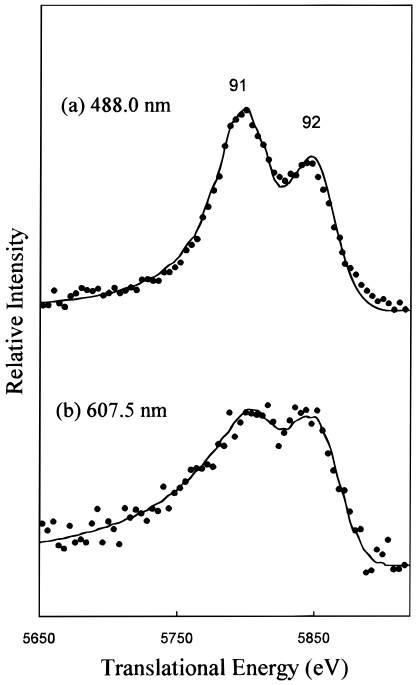

Figure 2. PD-MIKE spectra for dissociation of *n*-butylbenzene ion obtained at 1.5 kV applied on the electrode assembly: (a) 488.0 and (b) 607.5 nm excitations. Experimental and calculated results are shown as filled circles and solid curves, respectively. *m/z* of the fragment ion corresponding to each peak is indicated.

the lifetime is longer in the former. Relative abundances of the *m/z* 91 and 92 ions can not be determined readily from the field-on PD-MIKE spectra, however, because the two peaks are not well resolved. At the three excitation wavelengths used in this work, the combined intensities of the *m/z* 91 and 92 ions were ∼90% of the total daughter ion yields. The remainder was mostly due to the *m/z* 105 peak, which was not useful for kinetic analysis because of a poor signal-to-noise ratio. The

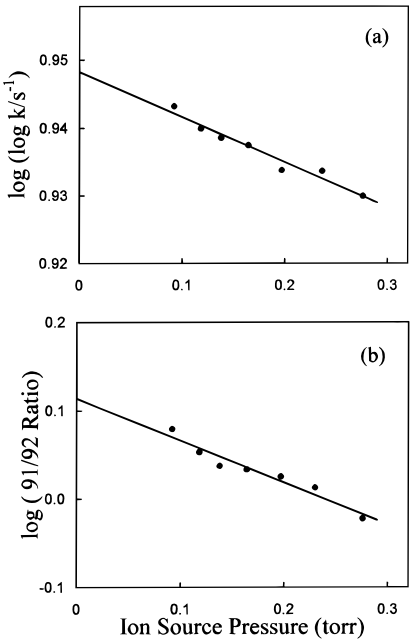

Figure 3. Plots of (a) log (log *k*) and (b) log (91/92 ratio) vs the pressure of the reagent gas in the ion source used for charge exchange ionization; 488.0 nm excitation. Filled circles represent experimental data. The solid lines are obtained from linear regression of experimental data.

method to determine the 91/92 ratio and the photodissociation rate constant simultaneously via peak shape analysis is described below.

The PD-MIKE peak shapes can be analyzed as described in detail previoulsy,[6,10] the only difference being that overlapping of peaks from two channels instead of one should be taken into account. The overall PD-MIKE peak shape obtained with an applied voltage is expressed as a weighted sum of $h(K;t)$, which is the peak shape function for the dissociation occurring at time t.

$$H(K) = \int P(t)\, h(K;t)\, \mathrm{d}t \qquad (3)$$

Here, K is the translational energy scale in the MIKE spectrum and $P(t)$ is the probability density for dissociation at time t. The relation between $P(t)$ and the rate constant distribution was described previously.[10] Then, the latter can be determined via regression. The PD-MIKE contour to be analyzed here consists of two peaks, *m/z* 91 and 92, and this fact must be incorporated into eq 3. It will be assumed that $P(t)$ is the same for the two reaction channels, which means that the two reactions occur competitively. This assumption will be further discussed later. Then, taking the 91/92 ratio, β, as an adjustable parameter, the following expression for $h(K;t)$ has been used.

$$h(K;t) = h_{92}(K;t) + \beta h_{91}(K;t) \qquad (4)$$

$h_i(K;t)$ is the normalized peak shape function for dissociation to m_i/z ion at time t, which can be estimated from the corresponding field-off spectrum. After determining β and rate constant distribution via regression, the peak contour was recalculated. For example, the recalculated contours are shown in Figure 2, a and b, demonstrating successful analyses. The 91/92 ratios in these cases are 1.20 and 0.50, respectively, and the average rate constants evaluated from the distributions are 6.0×10^8 and 1.3×10^8 s^{-1}. The internal energy distribution originating from the thermal energy necessitates the use of a distribution rather than a single value of the rate constant, which will be discussed later.

TABLE 1: The 91/92 Branching Ratios and Dissociation Rate Constants Derived from PD-MIKES Peaks

			rate constant (10^8 s^{-1})		
λ^a (nm)	E^b (eV)	91/92 ratio	total^c	*m/z* 91^d	*m/z* 92^e
607.5	3.71	0.72 ± 0.16	1.8 ± 0.5	0.68 ± 0.25	0.94 ± 0.35
514.5	4.08	1.15 ± 0.10	5.9 ± 1.0	2.8 ± 0.6	2.5 ± 0.5
488.0	4.21	1.30 ± 0.10	7.5 ± 1.6	3.8 ± 1.0	2.9 ± 0.8

[a] Photodissociation wavelength. [b] Average internal energy of the molecular ion after absorption of a photon. [c] Average total dissociation rate constant. [d] Average rate constant for the production of $C_7H_7^+$. [e] Average rate constant for the production of $C_7H_8^{\bullet+}$.

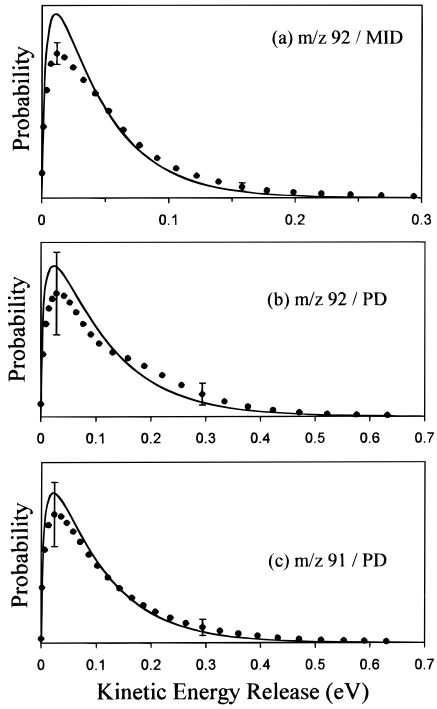

Figure 4. Kinetic energy release distributions in dissociation of *n*-butylbenzene ion: (a) metastable ion decomposition to $C_7H_8^{\bullet+}$; photodissociation to (b) $C_7H_8^{\bullet+}$ and (c) $C_7H_7^+$ at 488.0 nm. Experimental results are shown as filled circles. Theoretical (phase space theory) are shown as solid curves. Bars represent error limits.

In our previous photodissociation studies, [10,11,13] lowering of the internal energy of the molecular ions due to collisional relaxation in the ion source was observed and a method was devised to correct for its influence on the measured rate constant. Following the same procedure, the collisional relaxation-free rate constant was estimated by extrapolating the high-pressure data to the zero-pressure limit. An example is shown in Figure 3a for a set of rate constant data obtained at 488.0 nm. In addition to the rate constant, the 91/92 branching ratio has been found to depend on the ion source pressure also. A semi-log plot of the experimental ratio has been drawn as shown in Figure 3b and the collisional relaxation-free ratio has been estimated by linear extrapolation of the high-pressure data to the zero-pressure limit. The total rate constants and the 91/92 ratios thus obtained are summarized in Table 1. The individual rate constants for reactions 1 and 2 evaluated from their branching ratios and the total rate constants are also listed in the same table.

Kinetic energy release distributions (KERDs) have been determined from MIKE peak profiles using a well-established method.[29] For a more reliable determination of KERD in metastable ion decomposition (MID), a MIKE spectrum for MID occurring inside the cell located near the intermediate focal point has been obtained by floating the cell at high voltage (1.5 kV).[30]

TABLE 2: Thermochemical Data

species (structure)	ΔH°_{f298}[a] (kJ/mol)	ΔH°_{f0}[b] (kJ/mol)	IE[c] (eV)
n-$C_6H_5C_4H_9$	−13.2[d]	32[e]	8.66[e]
n-$C_6H_5C_4H_9^{\bullet+}$	822[e]	867[e]	
$C_6H_6CH_2^{\bullet+}$ (5-methylene-1,3-cyclohexadiene ion)	934[d]	957[f]	
	914[g]	937[f]	
$C_6H_5CH_2^{+}$ (benzyl ion)	897[h]	919[h]	
n-$C_3H_7^{\bullet}$	100.5[d]	115[d]	
	95.0[i]	109[f]	
	86.6[j]	101[f]	
C_3H_6 (propene)	20.2[d]	33[f]	

[a] Heat of formation at 298 K. [b] Heat of formation at 0 K. [c] Ionization energy. [d] Reference 31. [e] Reference 27. [f] Values converted from 298 K data. [g] Reference 21. [h] Reference 38. [i] Reference 39. [j] Reference 40.

The KERD in MID to *m/z* 92 ion thus determined is shown in Figure 4a. KERDs in photodissociation have been evaluated from field-off PD-MIKE spectra. The outer halves of the two MIKE peaks for *m/z* 91 and 92 ions have been used to minimize the interference between the two. KERDs in photodissociation were rather insensitive to the ion source pressure, making it unnecessary to correct for the collisional relaxation effect. KERDs in photodissociation to *m/z* 92 and 91 at 488.0 nm are shown in Figure 4, b and c, respectively.

4. Discussion

A. Internal Energy. The internal energy of the molecular ion generated by charge exchange ionization which was used in the photodissociation study is well approximated by[10]

$$E = \mathrm{RE} - \mathrm{IE} + E_{\mathrm{th}} \tag{5}$$

provided that collisional relaxation is not involved. Here, RE is the recombination energy of $CS_2^{\bullet+}$ and IE is the ionization energy for *n*-butylbenzene. Their best literature values are 10.07[31] and 8.66 eV,[27] respectively. (Thermochemical data are summarized in Table 2.) E_{th} is the thermal internal energy at 140 °C. Its distribution has been calculated with the molecular parameters in Table 3 as previously.[6] The internal energy distribution, $P_s(E)$, for the molecular ions in the ion source thus estimated is shown in Figure 5. Essentially all the molecular ions possess internal energies higher than the critical energy of ~1 eV[27] for reaction 1 which is the least endoergic channel. Hence, dissociation of some molecular ions during the flight between the ion source and the laser-ion beam crossing point will alter the internal energy distribution for the surviving molecular ions. This distribution for the molecular ions getting photoexcited can be estimated by the random lifetime distribution.[2]

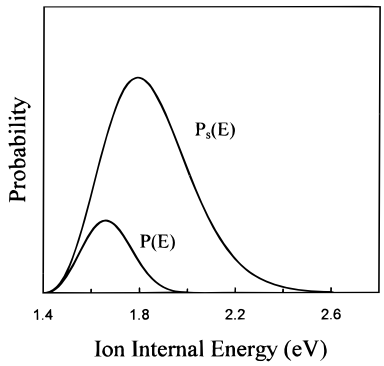

Figure 5. Internal energy distributions of *n*-butylbenzene ions in the ion source, $P_s(E)$, generated by charge exchange ionization and at the laser−ion beam crossing point, $P(E)$.

$$P(E) = P_{\mathrm{S}}(E)\exp[-k(E)\tau] \tag{6}$$

Here, τ is the flight time of the molecular ion to the laser-ion beam crossing point which is estimated to be 30 ± 2 μs at 8 keV acceleration energy in the ion source. The rate−energy dependence, $k(E)$, can be taken from the data reported by Baer et al.[27] $P(E)$ thus estimated is shown in Figure 5. The average internal energy evaluated from $P(E)$ is 1.67 eV. Adding the photon energy results in the average total internal energy of the photoexcited ion, which is 3.71, 4.08, and 4.21 eV at 607.5, 514.5, and 488.0 nm excitations, respectively. The average internal energy of the molecular ions undergoing MID has been estimated similarly,[7] which is 1.70 eV.

B. The 91/92 Branching Ratio. This ratio increases with the molecular ion internal energy according to all the previous investigations using various methods.[15−21,27] Among these previous reports, data obtained by Baer et al.[27] with PEPICO are thought to be the most reliable. The previous ion-beam photodissociation results[15] were reported as a function of the photon energy only, disregarding the internal energy of the molecular ions getting photoexcited. We also do not have much confidence in the charge exchange ionization results[19,20] because some needed calibrations such as the correction for the collisional relaxation were not made. The results from the PD-ICR work[21] agree reasonably well with the PEPICO results. The 91/92 ratios obtained in the present work are compared with

TABLE 3: Molecular Parameters Used in the Calculations of Thermal Energy Distribution, Rate Constants, and KERDs

	vibrational frequencies[a] (cm^{-1})	
n-$C_6H_5C_4H_9^{\bullet+}$[b]	3000(14), 1460(11), 1260(7), 1060(10), 910(6), 730(5), 590(2), 435(4), 265(4), 180, 90(2)	
$C_6H_5C_4H_9^{\bullet+}$ (TS1)[c]	3000(13), 1460(11), 1260(7), 1060(10), 910(6), 730(5), 590(2), 500(4), 340(4), 260, 135(2)	
$C_6H_5C_4H_9^{\bullet+}$(TS2)[d]	3000(14), 1460(11), 1260(7), 1060(10), 910(5), 730(5), 560(2), 320(4), 150(4), 120, 70(2)	
$C_7H_8^{\bullet+}$[e]	3010(8), 1510(6), 1240(7), 1010(7), 790(5), 570(2), 430(2), 340, 210	
$C_7H_7^{+}$[f]	2940(7), 1480(7), 1210(5), 1045(4), 940(4), 730(4), 485(4), 370	
n-$C_3H_7^{\bullet}$[g]	2930(7), 1420(6), 1250(3), 1080(2), 960(2), 860, 740, 340, 230	
C_3H_6[h]	3091, 3017, 2991, 2973, 2953, 2932, 1653, 1459,1443, 1419, 1378, 1298, 1174, 1045, 990, 945, 914, 912, 575, 428, 188	
	rotational constant[i] (cm^{-1})	polarizability[i] (10^{-24} cm^3)
n-$C_6H_5C_4H_9^{\bullet+}$	0.035	
$C_7H_8^{\bullet+}$	0.097	
$C_7H_7^{+}$	0.099	
n-$C_3H_7^{\bullet}$	0.441	5.8
C_3H_6	0.507	6.2

[a] Numbers in parentheses denote the degeneracies of vibrational modes. [b] Reference 27. [c] Transition state for the production of $C_7H_8^{\bullet+}$. [d] Transition state for the production of $C_7H_7^{+}$. [e] Values obtained from the frequencies for toluene from ref. 34. [f] Reference 38. [g] Values obtained from the frequencies for *n*-propyl halides from ref. 41. [h] Reference 35. [i] Estimated values.

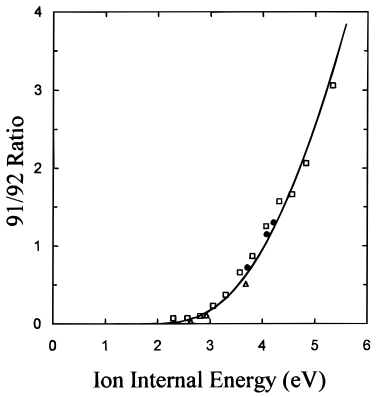

Figure 6. The 91/92 branching ratio as a function of *n*-butylbenzene ion internal energy. The present photodissociation results are shown as filled circles (●). The PEPICO results of Baer et al. (□) and PD-ICR results of Dunbar and co-workers (△) are also shown. The solid curve represents the theoretical result calculated from the rate−energy curves in Figures 7 and 8 at 298 K.

the PEPICO and PD-ICR data in Figure 6. The original PD-ICR data[21] reported by Dunbar and co-workers have been corrected for the thermal energy. Agreement among the data is remarkable considering that the three methods being compared operate on totally different principles. The results render a partial support to the general validity of the present PD-MIKES techniques, the method for the internal energy estimation in particular.

It has been generally accepted that the 91/92 ratios reported by Beynon and co-workers[15] in the photodissociation of *n*-butylbenzene ion generated by 70 eV electron ionization deviate from other results due to the neglect of the internal energy of the ion getting photoexcited. In this regard, we have measured the 91/92 ratios in PD-MIKES of molecular ions generated by 70 eV electron ionization also. These are 0.23, 0.54, and 0.66 at 607.5, 514.5, and 488.0 nm excitations, respectively. These values are smaller than reported by Beynon and co-workers. Such a difference is thought to arise from the fact that ions are irradiated perpendicularly near the intermediate focal point in the present experiment while the entire second field-free region was irradiated by Beynon and co-workers. Comparing the present results with the solid curve in Figure 6 which is the energy dependent 91/92 ratio obtained through RRKM-QET fitting to be described later, the average internal energies of 3.14, 3.60, and 3.74 eV are estimated for the photoexcited molecular ions with 607.5, 514.5, and 488.0 nm, respectively. (Since the solid curve has been estimated at 298 K, the additional rotational energy of 0.02 eV at 473 K, the ion source temperature in this photodissociation experiment, is added.) Then, subtracting the photon energies, the average internal energies of molecular ions getting photoexcited estimated from 607.5, 514.5, and 488.0 nm experiments become 1.10, 1.19, and 1.20 eV, respectively. The molecular ions getting photoexcited possess ∼1.16 eV of internal energy, the value being remarkably consistent in the three experiments. This suggests overall validity of the present method again. Also, this supports the argument that the neglect of the ion internal energy in the previous ion-beam photodissociation experiment was responsible for its mismatch with other data.

C. Production of $C_7H_8^{\bullet+}$. As was pointed out in an earlier section, the rate−energy dependence for this channel measured with PEPICO[27] required the participation of a tight transition state while the KERD measured by Holmes and Osborne[28] indicated dissociation via a loose transition state. To accommodate these apparently conflicting results, Baer et al. suggested that the reaction occur by the stepwise MaLafferty rearrangement via a distonic ion intermediate (DII) as shown in Scheme 1. The reaction occurs on a double-well potential energy surface, the first step being rate-determining while the second step determines the KERD.

As the first step to investigate the dynamics of this reaction, the KERD determined in this work is compared with the prediction from a statistical theory. The phase space theory formalism[32] which is easily applicable to dissociation occurring via a loose transition state without a reverse barrier would be adequate for this purpose.

$$n(T;J,E) \propto \int_{R_m}^{E-E_0-T} \rho(E - E_0 - T - R)P(T,J,R)\,\mathrm{d}R \quad (7)$$

Here, $n(T;J,E)$ is the KERD at a given angular momentum J and internal energy E. The root-mean-square average J value evaluated at the ion source temperature has been used.[33] ρ and P are the product vibrational and angular momentum state densities, respectively. R is the product rotational energy and R_m is its minimum. E_0 is the reaction critical energy which may be set equal to the reaction endoergicity at 0 K under the assumption of an extremely loose transition state. According to Scheme 1, 5-methylene-1,3-cyclohexadiene ion and propene are the reaction products. The heat of formation of the ionic product is not well established. The values of E_0 estimated from two recent heats of formation data[21,31] (Table 2) are 1.07 and 1.27 eV. E_0 of 1.17 eV, average of the two, has been used in the present calculation. KERDs have been calculated at various internal energies and averaged over the internal energy distributions for the molecular ions undergoing MID and photodissociation, respectively. The molecular parameters[34,35] used in the calculations are listed in Table 3. Theoretical KERDs shown in Figure 4a,b agree with the experimental ones virtually within error limits, respectively. It is to be noted that rearrangement reactions usually display kinetic energy releases much larger than statistical predictions.[36] Hence, the above results indicate that the separation of the ionic and neutral products in reaction 1 occurs via a loose transition state without a significant reverse barrier over a microsecond to nanosecond time scale, in agreement with Scheme 1.

The rate constant for this reaction has been calculated with the RRKM-QET formalism.[2,3]

$$k(E) = \sigma \frac{W^{\ddagger}(E - E_0)}{h\rho(E)} \quad (8)$$

Here, ρ is the density of states of the reactant ion, $W^{\ddagger}$ is the state sum at the transition state, and σ is the reaction path degeneracy. Since the difference in the external rotational moments of inertia between the reactant and the transition state is generally ignored, the rotational energy has not been included in the estimation of the ion internal energy. In a usual RRKM fitting of rate−energy data for a particular channel, the critical energy and the activation entropy at 1000 K ($\Delta S^{\ddagger}$) are treated as two parameters to be adjusted.[37] These two parameters have been varied to fit both the present and PEPICO rate constant data. Assuming that the isomerization in Scheme 1 is the rate-determining step, a C−H stretching mode (3000 cm^{-1}) has been taken as the reaction coordinate and σ of 2 has been used. Even though Baer et al.[27] took a 910 cm^{-1} mode as the reaction

SCHEME 1

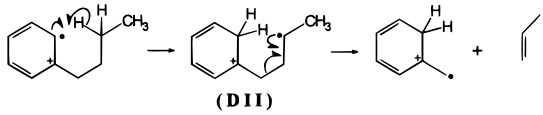

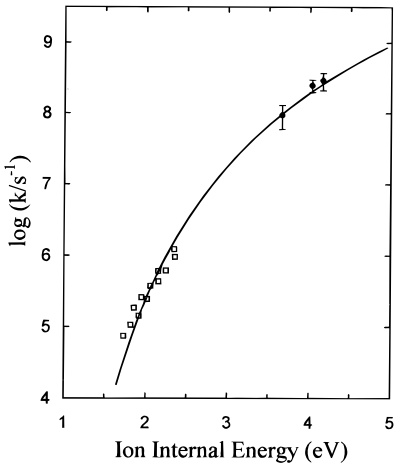

Figure 7. Rate−energy dependence for the dissociation of *n*-butylbenzene ion to $C_7H_8^{\bullet+}$. The present photodissociation results are shown as filled circles (●). The PEPICO results of Baer et al. (□) are also shown. The theoretical result (RRKM-QET) is shown as a solid curve. Rate parameters used in the calculation are $E_0 = 1.12$ eV and $\Delta S^{\ddagger} = -5.49$ eu. Bars represent error limits.

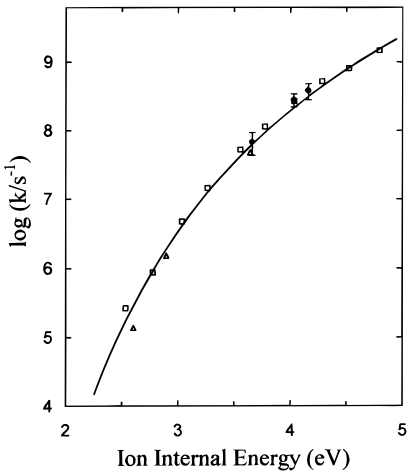

Figure 8. Rate−energy dependence for the dissociation of *n*-butylbenzene ion to $C_7H_7^+$. The present photodissociation results are shown as filled circles (●). The rate−energy data estimated from the curve in Figure 7 and the 91/92 ratios of Baer et al. (□) and Dunbar and co-workers (△) are also shown. The theoretical result (RRKM-QET) is shown as a solid curve. Rate parameters used in the calculation are $E_0 = 1.61$ eV and $\Delta S^{\ddagger} = 7.28$ eu. Bars represent error limits.

coordinate and used σ of 1, variation of these parameters has not been important. The best fit was achieved when E_0 of 1.12 eV and $\Delta S^{\ddagger}$ of −5.49 eu has been used, as shown in Figure 7. The vibrational frequencies used to achieve the above fit are listed in Table 3. The critical energy used is slightly larger than 0.99 eV adopted by Baer et al.[27] but is similar to 1.1 eV estimated by Dunbar and co-workers.[21] $\Delta S^{\ddagger}$ of −5.49 eu indicates that the reaction occurs via a tight transition state over the microsecond to nanosecond time scale. Conflicting indications from KERD and rate-energy data suggest the participation of a multiple-well potential in reaction 1, as shown in Scheme 1. $\Delta S^{\ddagger}$ of −10.9 eu reported by Baer et al. through RRKM-QET analysis of PEPICO data seems to be a little extreme compared to results in other rearrangement reactions. The value of the extended range made possible by our rates in the nanosecond region is clearly evident. Whereas the PEPICO data, covering only a 1 order of magnitude range of rates could not distinguish between $\Delta S^{\ddagger}$ of −11 and −5, the combined data, covering over 3 orders of magnitude in rate constants, permit us to establish a much more reliable entropy of activation. The internal energy distribution for the photoexcited molecular ion has been recalculated using the rate−energy relation obtained here. Its average is 0.01 eV larger than the previous estimation based on the rate data of Baer et al., which is negligible compared to the experimental error limits.

Accepting Scheme 1 for this reaction, E_0 of 1.12 eV obtained from RRKM-QET fit corresponds to the critical energy for the isomerization step. This value is comparable in magnitude to the endoergicity (1.07−1.27 eV) of the overall reaction. This means that the critical energies for the forward and backward reactions of the distonic ion intermediate are comparable, which, in turn, suggests the possibility of reversible occurrence of the first step in Scheme 1. Then, the measured rate constant may not correspond to the forward rate constant as assumed in the above analysis. Such a possibility will be probed later in this section after completing the analysis for reaction 2.

D. Production of $C_7H_7^+$. Unlike the production of $C_7H_8^{\bullet+}$, microsecond rate−energy data are not available for this channel. Using only the nanosecond data obtained in this work, however, may not allow a reliable RRKM-QET fitting. Hence, with the rate−energy curve for reaction 1 determined above and the branching ratios reported from PEPICO[27] and PD-ICR[21] studies, the rate constants for reaction 2 have been estimated over a wide internal energy range. These data are plotted in Figure 8 together with the nanosecond data obtained in this work. It is to be noted that the present data follow the same general trend as the PEPICO and PD-ICR data, supporting the overall validity of the present approach.

All the above data have been considered for RRKM-QET fitting for this reaction. The best fit was obtained when E_0 of 1.61 eV and $\Delta S^{\ddagger}$ of 7.28 eu were used, as shown in Figure 8. The C−C stretching mode at 910 cm^{-1} was taken as the reaction coordinate. The vibrational frequencies used in the calculation are listed in Table 3. The critical energy of 1.61 eV is the same as reported by Baer et al.[27] while $\Delta S^{\ddagger}$ is larger than 3.5 eu reported by these investigators. $\Delta S^{\ddagger}$ of 7.28 eu obtained in this work indicates that the reaction occurs via a very loose transition state by a simple bond cleavage and the most likely products, at least initially, are benzyl ion and *n*-propyl radical. For such a reaction, the critical energy will approach the reaction endoergicity very closely. The thermochemical data for the above products are not well established. The reaction endoergicity estimated from the thermochemical data[31,38−40] in Table 2 varies in the range 1.59−1.73 eV. E_0 of 1.61 eV determined in this work compares very well with the thermochemical data and is in excellent accord with the large value of $\Delta S^{\ddagger}$.

For a simple bond cleavage occurring statistically via a very loose transition state without a significant reverse barrier, the phase space theory is expected to provide a good description for KERD. The molecular parameters[38,41] used in the calculation are listed in Table 3. KERD in photodissociation is in excellent agreement with the calculated result as shown in Figure 4c.

E. A Stepwise McLafferty Rearrangement Mechanism. As was mentioned earlier, the isomerization step in the McLafferty rearrangement can occur reversibly and it is necessary to study how this affects the data analysis described above. The kinetic scheme for the major reactions investigated so far can be written as follows. The expressions for the rates

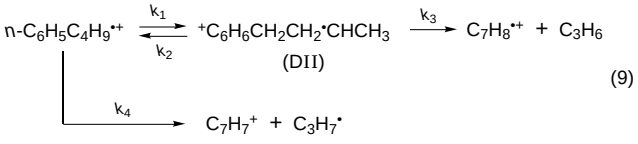

(9)

of production of $C_7H_8^{\bullet+}$ and $C_7H_7^+$ can be found elsewhere[42]

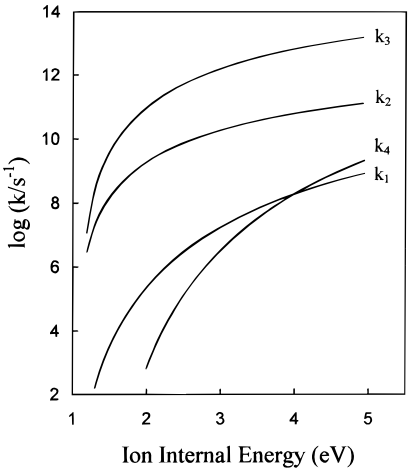

Figure 9. Rate−energy dependences for the four channels in reaction 9. See text for details.

and can be written as below if DII is not present initially.

$$\frac{d[C_7H_8^{\bullet+}]}{dt} = \frac{k_1k_3}{\lambda_+ - \lambda_-}(e^{-\lambda_- t} - e^{-\lambda_+ t}) \quad (10)$$

$$\frac{d[C_7H_7^{+}]}{dt} = \frac{k_4}{\lambda_+ - \lambda_-}[(\lambda_+ - k_1 - k_4)e^{-\lambda_- t} - (\lambda_- - k_1 - k_4)e^{-\lambda_+ t}] \quad (11)$$

where

$$\lambda_\pm = {}^1/_2[(k_1 + k_2 + k_3 + k_4) \pm \sqrt{(k_2 + k_3 - k_1 - k_4)^2 + 4k_1k_2}] \quad (12)$$

To arrive at simplified versions of the above rate equations applicable to the present case, it is necessary to have estimates of the magnitudes of k_1, k_2, k_3, and k_4. k_1 and k_4 have been evaluated already in this work, namely the rates of production of $C_7H_8^{\bullet+}$ and $C_7H_7^{+}$, respectively. To evaluate k_2 and k_3, thermochemical and structural information on DII is needed. According to Kuck,[43] the heat of formation at 298 K of DII is roughly 887 kJ/mol which is ~65 kJ/mol higher than that of the *n*-butylbenzene ion. The critical energies for the reverse isomerization and dissociation of DII evaluated from this value are 0.45 and 0.50 eV, respectively. Since $\Delta S^{\ddagger}$ is mostly determined by the tightness (or looseness) of the transition state, it seems to be reasonable to use −5.49 eu in the calculation of k_2, which is the same value used for k_1. Since the dissociation of DII is presumed to occur via a very loose transition state as indicated by KERD analysis, $\Delta S^{\ddagger}$ of 7.28 eu, which is the value used for k_4, has been adopted for k_3. The rate−energy relations $k_1(E)$−$k_4(E)$ are shown in Figure 9. At the internal energy range investigated by PEPICO, PD-ICR, and the present PD-MIKES technique, the relation k_1, $k_4 \ll k_2 \ll k_3$ holds. In this limiting case, eqs 10 and 11 are simplified as below.

$$\frac{d[C_7H_8^{\bullet+}]}{dt} \approx k_1 \exp[-(k_1 + k_4)t)] \quad (13)$$

$$\frac{d[C_7H_7^{+}]}{dt} \approx k_4 \exp[-(k_1 + k_4)t)] \quad (14)$$

That is, the appearance rates of $C_7H_7^{+}$ and $C_7H_8^{\bullet+}$ are determined by $k_1 + k_4$ and their branching ratio by k_4/k_1, in agreement with the kinetic treatment made in this work and by Baer et al. It is to be noted that the above simple treatment is not generally applicable to competing consecutive reactions. For example, if DII is more stable than estimated by Kuck, the above limiting situation may not hold especially in a low internal energy region. Then, k_1 and/or k_4 cannot be determined from the experimental rates without the knowledge of k_2 and k_3.

5. Conclusions

Photodissociation of *n*-butylbenzene ion has been found to occur competitively to $C_7H_8^{\bullet+}$ and $C_7H_7^{+}$ on a nanosecond time scale. The transition state structures inferred from the measured rate−energy relation and the KERD for the production of $C_7H_8^{\bullet+}$ were different. The controversy could be resolved by assuming that the reaction occurs consecutively via a distonic ion intermediate, in agreement with Baer et al.[27] The reaction seems to be a stepwise McLafferty rearrangement in which isomerization via a γ-hydrogen rearrangement is followed by α-cleavage to 5-methylene-1,3-cyclohexadiene ion and propene. On the other hand, the production of $C_7H_7^{+}$ which is dominant at higher internal energy occurs by a simple bond cleavage to benzyl ion and *n*-propyl radical.

Combining previous microsecond rate−energy data and the branching ratios with the nanosecond data, RRKM-QET fitting could be improved as manifested by more reasonable values of $\Delta S^{\ddagger}$. Successful analysis with the statistical theories also means that the dissociation occurs on the potential energy surface of the ground electronic state even though photoabsorption initially leads to an excited electronic state(s). The quasi-equilibrium hypothesis generally made for the dissociation of polyatomic ions seems to hold in this case. This is in contrast with the photodissociation of one of its isomers, *tert*-butylbenzene ion, which displayed apparent non-RRKM-QET behavior.[12]

The excellent agreement of the 91/92 ratio determined in this work with the previous PEPICO and PD-ICR results indicates the overall validity of the present PD-MIKES technique, the method for the internal energy estimation in particular. Also, this is the first time that overlapping PD-MIKE peaks arising from two competing channels have been successfully analyzed.

Acknowledgment. This work was supported financially by the Ministry of Education, Republic of Korea, by Center for Molecular Catalysis and Korea Science and Engineering Foundation, and by the Non Directed Research Fund, Korea Research Foundation.

References and Notes

(1) Levsen, K. *Fundamental Aspects of Organic Mass Spectrometry*; Verlag Chemie: Weinheim, Germany, 1978.

(2) Forst, W. *Theory of Unimolecular Reactions*; Academic Press: New York, 1973.

(3) Robinson, P. J.; Holbrook, K. A. *Unimolecular Reactions*; Wiley-Interscience: New York, 1972.

(4) Baer, T. *Adv. Chem. Phys.* **1986**, *64*, 111. Booze, J. A.; Schweinsberg, M.; Baer, T. *J. Chem. Phys.* **1993**, *99*, 4441. Riley, J.; Baer, T. *J. Phys. Chem.* **1993**, *97*, 385. Booze, J. A.; Feinberg, T. N.; Keister, J. W.; Baer, T. *J. Chem. Phys.* **1994**, *100*, 4294.

(5) Dunbar, R. C. *J. Phys. Chem.* **1987**, *91*, 2901. Gotkis, Y.; Naor, M.; Laskin, J.; Lifshitz, C.; Faulk, J. D.; Dunbar, R. C. *J. Am. Chem. Soc.* **1993**, *115*, 7402. Lin, C, Y.; Dunbar, R. C. *J. Phys. Chem.* **1994**, *98*, 1369. Weddle, G. H.; Dunbar, R. C.; Song, K.; Morton, T. H. *J. Am. Chem. Soc.* **1995**, *117*, 2573.

(6) Choe, J. C.; Kim, M. S. *J. Phys. Chem.* **1991**, *95*, 50.

(7) Choe, J. C.; Kim, M. S. *Int. J. Mass Spectrom. Ion Processes* **1991**, *107*, 103.

(8) Choe, J. C.; Kim, M. S. *J. Phys. Chem.* **1992**, *96*, 726.

(9) Yim, Y. H.; Kim, M. S. *Int. J. Mass Spectrom. Ion Processes* **1993**, *123*, 133.
(10) Yim, Y. H.; Kim, M. S. *J. Phys. Chem.* **1993**, *97*, 12122.
(11) Yim, Y. H.; Kim, M. S. *J. Phys. Chem.* **1994**, *98*, 5201.
(12) Cho, Y. S.; Choe, J. C.; Kim, M. S. *J. Phys. Chem.* **1995**, *99*, 8645.
(13) Cho, Y. S.; Kim, M. S.; Choe, J. C. *Int. J. Mass Spectrom. Ion Processes* **1995**, *145*, 187.
(14) Hwang, W. G.; Kim, M. S.; Choe, J. C. *J. Phys. Chem.* **1996**, *100*, 9227.
(15) Mukhtar, E. S.; Griffiths, I. W.; Harris, F. M.; Beynon, J. H. *Int. J. Mass Spectrom. Ion Phys.* **1981**, *37*, 159.
(16) Griffiths, I. W.; Mukhtar, E. S.; March, R. E.; Harris, F. M.; Beynon, J. H. *Int. J. Mass Spectrom. Ion Phys.* **1981**, *39*, 125.
(17) Griffiths, I. W.; Mukhtar, E. S.; Harris, F. M.; Beynon, J. H. *Int. J. Mass Spectrom. Ion Phys.* **1982**, *43*, 283.
(18) Welch, M. J.; Pereles, D. J.; White, E. *Org. Mass Spectrom.* **1985**, *20*, 425.
(19) Harrison, A. G.; Lin, M. S. *Int. J. Mass Spectrom. Ion Phys.* **1983**, *51*, 353.
(20) Nacson, S.; Harrison, A. G. *Int. J. Mass Spectrom. Ion Processes* **1985**, *63*, 325.
(21) Chen, J. H.; Hays, J. D.; Dunbar, R. C. *J. Phys. Chem.* **1984**, *88*, 4759.
(22) Uechi, G. T.; Dunbar, R. C. *J. Chem. Phys.* **1990**, *93*, 1626.
(23) Uechi, G. T.; Dunbar, R. C. *J. Chem. Phys.* **1993**, *98*, 7888.
(24) McLuckey, S. A.; Sallans, L.; Cody, R. B.; Burnier, R. C.;Verma, S.; Freiser, B. S.; Cooks, R. G. *Int. J. Mass Spectrom. Ion Phys.* **1982**, *44*, 215.
(25) Dawson, P. H.; Sun, W. F. *Int. J. Mass Spectrom. Ion Phys.* **1982**, *44*, 51.
(26) Waddell, D. S.; Boyd, R. K.; Brenton, A. G.; Beynon, J. H. *Int. J. Mass Spectrom. Ion Processes* **1986**, *68*, 71.
(27) Baer, T.; Dutuit, O.; Mestdagh, H.; Rolando, C. *J. Phys. Chem.* **1988**, *92*, 5674.
(28) Holmes, J. L.; Osborne, A. D. *Org. Mass Spectrom.* **1981**, *16*, 236.
(29) Yeh, I. C.; Kim, M. S. *Rapid Commun. Mass Spectrom.* **1992**, *6*, 115; 293.
(30) Kim, Y. H.; Kim, M. S. *Rapid Commun. Mass Spectrom.* **1991**, *5*, 25.
(31) Lias, S. G.; Bartmess, J. E.; Liebman, J. F.; Holmes, J. L.; Levin, R. D.; Mallard, W. G. *J. Phys. Chem. Ref. Data* **1988**, *17*, Suppl. 1.
(32) Chesnavich, W. J.; Bowers, M. T. In *Gas Phase Ion Chemistry*; Bowers, M. T., Ed.; Academic Press: New York, 1979; Vol. I, Chapter 4. Chesnavich; W. J.; Bowers, M. T. *Prog. React. Kinet.* **1982**, *11*, 137.
(33) Choe, J. C.; Kim, B. J.; Kim, M. S. *Bull. Korean Chem. Soc.* **1989**, *10*, 167.
(34) Draeger, J. A. *Spectrochim. Acta* **1985**, *41A*, 607.
(35) Dewar, M. J. S.; Ford , G. P. *J. Am. Chem. Soc.* **1977**, *99*, 1685.
(36) Lee, T. G.; Park, S. C.; Kim, M. S. *J. Chem. Phys*., in press.
(37) Lifshitz, C. *Adv. Mass Spectrom.* **1989**, *11*, 713.
(38) Baer, T.; Morrow, J. C.; Shao, J. D.; Olesik, S. *J. Am. Chem. Soc.* **1988**, *110*, 5633.
(39) Holmes, J. L.; Lossing, F. P.; Maccoll, A. *J. Am. Chem. Soc.* **1988**, *110*, 7339.
(40) Rosenstock, H. M.; Draxl, K.; Steiner, B. W.; Herron, J. T. *J. Phys. Chem. Ref. Data* **1977**, *6*, Suppl. 1.
(41) Shimanouchi, T.; Matsuura, H.; Ogawa, Y.; Harada, I. *J. Phys. Chem. Ref. Data* **1978**, *7*, 1323.
(42) Baer, T.; Brand, W. A.; Bunn, T. L.; Butler, J. J. *Faraday Discuss. Chem. Soc.* **1983**, *75*, 45.
(43) Kuck, D. *Mass Spectrom. Rev.* **1990**, *9*, 187.

JP9605818